Boundary Element Method Macromodels for 2-D Hierarchical Capacitance Extraction†

E. Aykut Dengi
Motorola Inc.
3501 Ed Bluestein Blvd., Austin, TX 78721

Ronald A. Rohrer
Intersouth Partners
1000 Park Forty Plaza, RTP, NC 27709

Abstract

A 2-D hierarchical field solution method was recently introduced for capacitance extraction for VLSI interconnect modeling. In this paper, we present several extensions to the method including a Boundary Element Method (BEM) formulation for creating macromodels, which provides a better trade-off between accuracy and efficiency, as well as parameterized elements, which allow the analysis of gridless designs with reasonable accuracy and a small library size.

1. Introduction

Capacitance extraction is a critical step in submicron integrated circuit interconnect modeling. In [4] a hierarchical 2-D capacitance extraction method for VLSI circuits was introduced. The method uses a geometrical hierarchical partitioning on the 2-D vertical cross-section of a VLSI circuit. These partitions are characterized at their interfaces by macromodel capacitance matrices which can be combined to yield a global capacitance matrix for a given set of conductors or the coupling capacitance values for a given conductor (Fig. 1). A library of such macromodels, which is sufficient to describe any vertical cross section for a given technology, is built as a pre-processing step to improve runtime extraction efficiency. Irregular conductor geometries as well as conformal dielectrics are handled at the preprocessing stage, enhancing runtime efficiency without affecting accuracy.

To aid understanding, [4] introduced the method in a Finite Difference Method formulation, but the method is in fact best implemented using the Boundary Element Method (BEM). The efficiency of the runtime global solution is proportional to the number of ports on each element. In the finite difference formulation, the number of ports is intimately related to the discretization used inside the element. Hence, when we discretize the conductor surfaces finely, as we should, we end up with a large number of ports. In this paper, we present the BEM formulation, which allows us to effectively decouple the discretization on the conductors and the discretization at the boundary (hence the number of ports), leading to a better trade-off between accuracy and efficiency.

The rest of the paper is organized as follows: In Section 2, the basic BEM formulation for macromodels is presented; Section 3 describes how these macromodels can be combined to yield capacitance values for a given configuration of conductors; Section 4 discusses how the choice of different interpolation functions for the BEM affects accuracy and efficiency; Section 5 presents how a versatile library can be built as a pre-processing step for maximum efficiency and accuracy; Finally in Section 6, we offer some conclusions.

†. This work was supported by the National Science Foundation under Grant MIP-9216942, and by the Semiconductor Research Corporation under Contract DC-068.

2. BEM Formulation

With BEM we attain the most accuracy for a given number of nodes, because no error is incurred inside the domain being analyzed and all the error is due to the approximation of flux density and potential at the boundaries of the domain. The inside of the domain need not be discretized using the BEM [2]. In the traditional use of the method, there is a performance penalty due to two factors: BEM gives rise to a full matrix, and it is expensive to calculate the entries of this matrix and to invert it. In our methodology, however, some of these expenses are all shifted to the pre-processing library building phase where they can be afforded, as we shall see below.

The BEM relates the potential at the conductor boundaries to the charge distribution at those boundaries. However, in order to repeat what we did with Finite Differences, using the BEM we must artificially partition the problem domain into cells to be characterized separately. In FD, we chose points that already existed in the grid for the FD solution and created a boundary. In BEM, however, there are no nodes in the dielectric between conductors, so we must create them artificially. In this case, we have not only the charge distribution on conductors, but also the flux density at the artificial interfaces created.

The creation of such artificial boundaries may seem redundant, or even detrimental to accuracy at first. However, we have reasons to believe that we may gain by using our method as opposed to a straight forward BEM implementation:

1. The charge density in the regular BEM varies rapidly near conductor corners, necessitating more nodes, whereas potential and flux density vary smoothly at the artificial boundaries we have chosen so that fewer nodes suffice;
2. In regular BEM, it is not possible to form the potential matrix [9] as a pre-processing step, and it is very costly at run-time, therefore macromodeling is not possible;
3. Regular BEM generates dense potential matrices to be inverted,

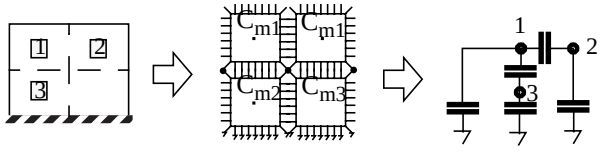

Figure 1. Hierarchical field solution combines the individual macromodels eliminating nodes at their common edges.

1-58113-049-x-98/0006/$3.50

whereas our method generates block-sparse matrices;

4. BEM can handle only absorbing boundary conditions, which may not be appropriate to the problem domain.

Such partitioning of the problem domain using the BEM, referred to as multi-zone BEM, has been used in mechanics [7] and the capacitance extraction of SRAM cell vertical cross-sections [5]. [7] uses the multi-zone BEM method on elasticity problems. [5] uses the multi-zone BEM to model multiple dielectric layers (assigning them to different zones) and to break up zones with large aspect ratios, which tend to cause numerical problems, into sections with smaller aspect ratios. Both references compute the entries of the global capacitance (using Green's functions) matrix at runtime and do not consider macromodeling. We give a brief summary of the DBEM as used by our method below. Detailed background can be found in, e.g.,[2].

For any point x at the boundary G (Fig. 2), the following equations hold [2]:

$$c(\xi)u_0(\xi) + \int_\Gamma u_0(x)\, f^*(\xi, x)d\Gamma(x) = \int_\Gamma f_0(x)u^*(\xi, x)d\Gamma(x) \tag{1}$$

$$u^*(\xi, x) = \frac{1}{2\pi} ln\left(\frac{1}{r(\xi, x)}\right) \tag{2}$$

$$f^*(\xi, x) = \frac{\partial}{\partial n} u^*(\xi, x)\,. \tag{3}$$

If the boundary is smooth, $c(\xi) = 1/2$. We pick N collocation points ξ on Γ and use the subscript i to mark the quantities at ξ_i, as in Fig. 2. We use the same set of interpolation functions ϕ to approximate u_0 and f_0:

$$u_0 \cong u = \sum_{k=1}^{N} \phi_k u_k\,,\ f_0 \cong f = \sum_{k=1}^{N} \phi_k f_k \tag{4}$$

We may further pick interpolation functions such that

$$\phi_k(x) = 0 \text{ if } x \notin \Gamma_k\,,\ k \in \{1, 2 \ldots N\} \tag{5}$$

where Γ_k are segments such that

$$\bigcup_k \Gamma_k = \Gamma \text{ and } \xi_k \in \Gamma_k \tag{6}$$

Then, we can write Eq. (1) in matrix form:

$$Hu = Gf\,,\ H_{ij} = c_i\delta_{ij} + \int_{\Gamma_j} \phi_j(x)\, f^*(\xi_i, x)d\Gamma(x)\,,$$

$$G_{ij} = \int_{\Gamma_j} \phi_j(x)u^*(\xi_i, x)d\Gamma(x) \tag{7}$$

where $c_i = 1/2$ for smooth boundaries. And finally,

$$C = G^{-1}H \tag{8}$$

This C matrix contains all the individual nodes on the boundary and the conductors. We condense the conductor nodes into one

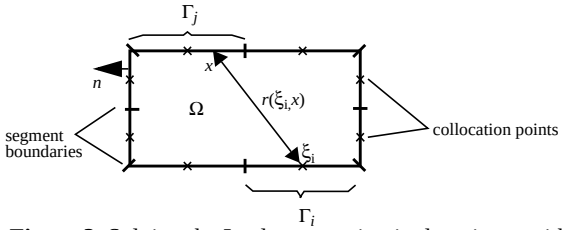

Figure 2. Solving the Laplace equation in domain Ω with boundary Γ using the BEM. For constant elements, the collocation point is in the middle of each segment.

without loss of accuracy by integrating the flux f on each conductor to calculate q, the total charge on that conductor:

$$C_m = RCP^T\,,\ R = \begin{bmatrix} I_n & 0 \\ 0 & R_c \end{bmatrix}\,,\ r_i = \int_\Gamma \phi_i(x)d\Gamma(x)\,, \tag{9}$$

$$R_{c(\text{k x (N-n)})} = \begin{bmatrix} r_{n+1} & r_{n+2} & \cdots & r_{n+l_1} & 0 & \cdots & 0 & 0 & \cdots & 0 & 0 \\ 0 & 0 & 0 & 0 & r_{n+l_1+1} & \cdots & r_{n+l_1+l_2} & 0 & \cdots & 0 & 0 \\ 0 & \cdots & \cdots & \cdots & \cdots & \cdots & \cdots & \cdots & \cdots & 0 & 0 \\ 0 & \cdots & \cdots & \cdots & \cdots & \cdots & \cdots & \cdots & \cdots & \cdots & r_N \end{bmatrix} \tag{10}$$

where n is the number of terminals on the boundary, k is the number of conductors in the macro l_i is the number of nodes on the ith conductor and r_i is the total charge on the segment i. P is defined as:

$$P = \begin{bmatrix} I & 0 \\ 0 & P_c \end{bmatrix}\,,\ P_c = p_{ij}$$

$$p_{ij} = \begin{cases} 1 & \text{if node j is on conductor i} \\ 0 & \text{otherwise} \end{cases} \tag{11}$$

We can now partition C_m:

$$C_\text{m} v = \begin{bmatrix} C_{bb} & C_{bc} \\ C_{cb} & C_{cc} \end{bmatrix} \begin{bmatrix} v_b \\ v_c \end{bmatrix} = \begin{bmatrix} f_b \\ q_c \end{bmatrix} \tag{12}$$

where subscript b denotes nodes on the artificial boundary, subscript c denotes nodes corresponding to each conductor inside the macromodel, v denotes potentials at nodes/conductors, f denotes flux density at nodes and q denotes total charge on conductors

3. Global Solution

We obtain a global solution using BEM macromodels in much the same as with FD macromodels in [4]. We stencil the macromodel of each element into a global capacitance matrix and eliminate the nodes at the interfaces between elements through a partial LU-decomposition:

$$C = C_{22} - C_{21}C_{11}^{-1}C_{12}\,, \tag{13}$$

where the subscript 1 indicates the nodes that are eliminated and the subscript 2 the nodes that remain. Using Eqn. (13), we can obtain a capacitance matrix for a set of conductors; alternatively, we can obtain a macromodel for the given configuration by preserving the nodes at the outer boundary of the configuration.

Because the individual library elements are built *a priori*, the conductors and dielectric interfaces inside an element macromodel can be discretized as finely as needed without increasing the size of C_m. Thus, more time can be spent during pre-processing for condensing the conductor nodes and eliminating the inner dielectric interface nodes. This improves the accuracy of the macromodel by arbitrarily reducing the error due to the discretization of the conductors without having a negative impact on subsequent extraction runtime.

4. Order of Interpolation Functions

In Eq. (4), we specify a set of interpolating functions, but we so far have not discussed how the choice of such functions affects our

method. The most common interpolation function is zeroth-order piecewise constant. It has been used extensively and with success in conjunction with the Indirect (or regular) BEM (IBEM). One reason for its common use is the ease of implementation. The integrals used in the construction of matrices *H* and *G* become more complicated as the order of the interpolation function increases. However, it is also well-known that higher-order interpolation functions lead to a higher rate of asymptotic convergence for Direct BEM (DBEM) methods [10]†.

Comparisons of different interpolation functions have been carried out in literature for the DBEM in general (see, for instance, [10]), and specifically for our method in [3]. Here, we will illustrate the convergence peoperties of different interpolation functions on an example. The configuration in Fig. 3 is solved with constant, linear partially discontinuous, linear discontinuous and quadratic elements. The convergence of each is graphed in Fig. 4. The number of nodes per element is determined by the discretization at the boundary of the element (Fig. 3b) and is a good measure of the efficiency of the solution because it determines the size of the global capacitance matrix. The dashed lines in the logarithmic plots are inserted for reference. The absolute value of the slope of an error curve is equal to the order of the asymptotic convergence for the corresponding method. The discretization *dm* for the conductors inside the elements (see Fig. 3b) affects the accuracy but does not have an effect on the efficiency of the global solution. For the results in Fig. 4, $dm = 0.05$.

We see that in terms of asymptotic convergence, quadratic elements have the best properties. However, in IC applications, we are not really after errors on the order of 10^{-4}, because we know that our geometrical parameters and the process variations present much greater variations. Therefore asymptotic convergence is of limited use in a practical application. We are more interested in which method yields a given accuracy most economically. We can attain reasonable accuracy (~1%) for the lowest discretization for both diagonal and off-diagonal entries of the capacitance matrix. We also see that quadratic elements intrinsically have a larger minimum number of nodes per element. Experience suggests that in fact, the discontinuous linear elements offer good compromises among efficiency, accuracy and ease of implementation. As our method matures, higher orders of interpolation functions may prove in the future to provide better trade-offs.

The number of nodes on the conductor is not the only determinant of accuracy we can improve without a run-time performance

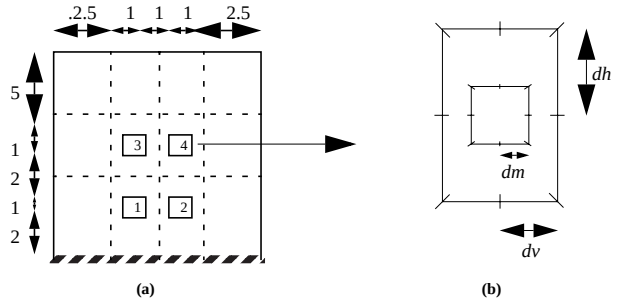

Figure 3. Example illustrating the convergence of different interpolating functions. (a) shows the dimensions of the configuration and (b) defines the variables for a single element

†. The difference between IBEM and DBEM is that only charge (or flux density) is discretized in the former and both flux density and potential in the latter.

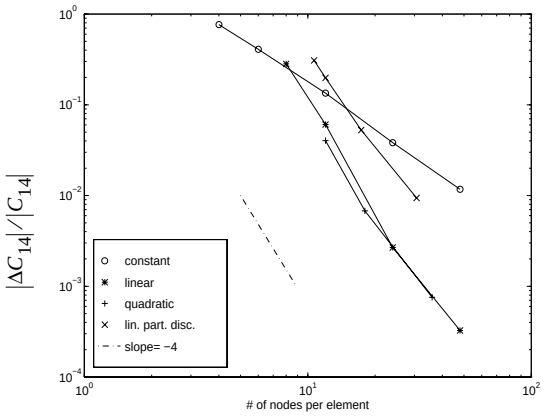

Figure 4. The relative error in one component of the capacitance matrix (C_{14}) for the configuration in Fig. 3is plotted for constant, discontinuous linear, partially discontinuous linear and quadratic elements for varying discretization.

penalty. In [5], the accuracy of integration (in the computation of the capacitance matrix elements) is identified as a major determinant of accuracy. Note that a high accuracy integration with many grid points on the conductor would be very costly if executed at run-time as in regular BEM [5]. Our method shifts this computational cost to pre-processing. The advantage of our method is more pronounced for more complicated conductor geometries.

In order to demonstrate this, we examine the simple problem in Fig. 5. An imaginary process with two distinct dielectric layers is modeled: layer 1 with a dielectric constant $\varepsilon = 1$ and layer 2 with $\varepsilon = 1.5$. The top metal layer has an irregular cross-section. Conductor 1 is slightly shifted to the right to render the problem non-symmetric. The relative error is expressed in percentages as $100(\left|C_x^{\text{approx}} - C_x^{\text{exact}}\right| / C_{11}^{\text{exact}})$ in Fig. 5(b). We see that even for a very coarse discretization (with a total of 30 nodes in the global solution) the error is below 1.5%.

5. Library Building

One of the advantages of the hierarchical field solution approach is that a significant part of the computational cost can be shifted to the pre-processing stage by building a library of macromodels which can be combined to describe any vertical cross-section allowed for a given technology [4]. Only three basic elements (Fig. 6) are sufficient to span each unique interconnect layer [4], but more complex elements may be added to the library for improved efficiency and accuracy. A detailed discussion on the tradeoffs between library size, efficiency and accuracy can be found in [3]. Here, we shall present two aspects of library building that prove to be crucial in practice: parameterized macromodels and interfacing macormodels with different discretizations.

Parameterized Macromodels

Instead of coming up with several unique elements for each conductor width, we can make the macromodel parameters of an element functions of the width of the conductor. We can do the same with respect to spacing between conductors as well. The macromodel capacitance matrices C_{m} in Fig. 6 may be general functions. However, a piecewise-linear function is often enough for accuracy because the range of parameters is limited. Moreover, the accuracy

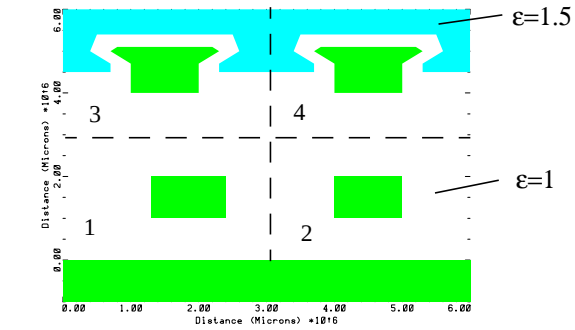

(a)

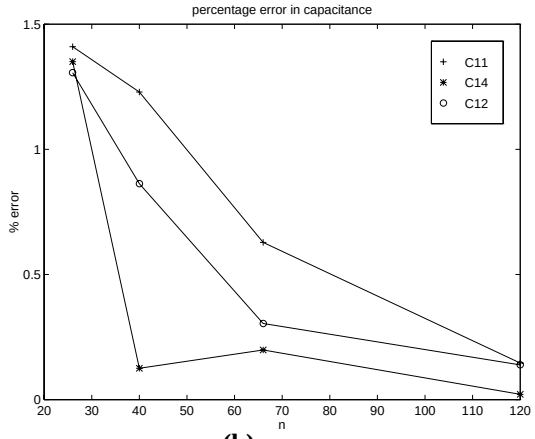

(b)

Figure 5. Convergence with improving discretization (a) The vertical cross-section for an imaginary process. The dielectric constant is taken as 1. The top metal layer has an irregular cross-section and there is a conformal dielectric with a dielectric constant 1.5. Dashed lines indicate the element boundaries used. (b) shows the convergence in absolute terms of C11, the total capacitance of conductor 1, and C14, the coupling capacitance between conductors 1 and 4. n is the number of variables in the global capacitance matrix formed.

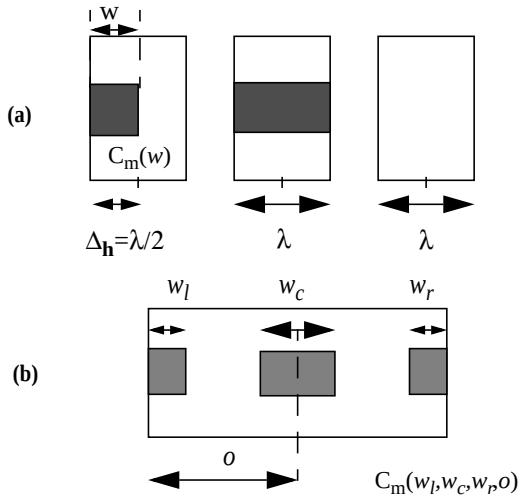

Figure 6. (a) The minimum set of three basic elements that span a layer of a given technology; **(b)** a complex element.

can be arbitrarily improved by increasing the number of segments and/or increasing the order of the interpolating function. In the case of one linear segment:

$$\bar{C}_{\mathrm{m}}(w) = \bar{C}_{\mathrm{m0}} + (w - w_0)\Delta C_w\,,\ w_{\min} < w < w_{\max}\,. \qquad (14)$$

$$\left|\bar{C}_{\mathrm{m}}(w) - C_{\mathrm{m}}(w)\right| < \varepsilon \qquad (15)$$

It is possible to use many numerical techniques to compute C_{m0} and ΔC_w, such as a least-squares fit, interpolation or analytic differentiation. It is always possible to pick w_{min}, w_{max} such that Eq. (15) holds. For large parameter variations and rapidly changing functions, this would mean that we would need more segments for a given error bound. Macromodel matrix functions of more than one variable (Fig. 6b) can be similarly handled.

By running many experiments [3], we have found that the parameterization error is insignificant (1-3%) and is dominated by the error due to the discretization of the boundaries for practical purposes. Complex elements (e.g., Fig. 6b) tend to decrease the error due to discretization and reduce the number of unknowns in the global solution matrix, resulting in high efficiency and accuracy. Therefore, there is a good reason to build a library of parameterized and possibly complex elements to minimize the number of interfaces between conductors while maintaining a reasonable library size.

Interfacing Elements with different discretizations

In defining library elements, we have imposed limitations so that all elements that can be neighbors have matching ports [4]. This is a significant limitation when we require a higher level of accuracy on the capacitance of some nets than others, e.g., in a net-by-net extraction methodology. We need a finer discretization closer to the net of interest (NOI) than farther away from it. However, the limitation that all elements have the same discretization does not allow us to use a coarser grid as we move away from the NOI. This causes inefficiency, especially for large problems. There are two solutions to this problem:

1. We can have elements with edges that have different discretizations. For instance, the left vertical edge of an element could have twice as many ports as the right vertical edge. We could use such an element with the left edge facing the NOI (Fig. 7). This solution results in a larger library because we now need to store *versions* of the same element, which have different discretizations.
2. We can try to interface elements with non-matching ports through interpolation. In classic BEM literature, this is not considered good practice [2], because BEM minimizes the error in potential and flux density at nodes. Therefore, the non-node parts of an element, of which interpolation would make use, may have larger errors.

We will describe the second approach because of its positive impact on performance. The essence of the problem is demonstrated in Fig. 8. As discussed above, given potential at ports, capaci-

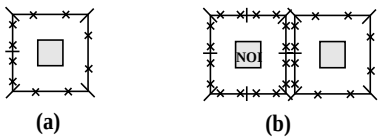

Figure 7. Elements with different discretization on different edges: **(a)** shows an element for which the left edge has a higher discretization; **(b)** shows this element used with the left edge facing the NOI, which has high discretization on all edges .

tance macromodel matrices yield flux density. We see that four ports of element one (E1) correspond to only two ports of element two (E2). We are trying to satisfy the compatibility conditions at the interface. Therefore, the potential (flux density) on E1 must be equal to the potential (flux density) on E2. We use a *least-squares* fit to obtain the potential on E2, v_2. Given v_2, C_2 yields f_2, which is supported by the two ports of E2. Linear interpolation is used to obtain f_1. By doing this, we constrain the degrees of freedom of f_1: The two segments are constrained to act as one. This is equivalent to a matrix transformation:

$$\boldsymbol{T}\text{:}\ C_2^{(2\times 2)} \rightarrow P^{(4\times 2)} C_2^{(2\times 2)} Q^{(2\times 4)} = \tilde{C}_2^{(4\times 4)} \tag{16}$$

which transforms C_2 into a 4x4 matrix, $\tilde{C}_2$, which is compatible with C_1 (Fig. 9(a)).

We shall examine an example that is in line with the net-by-net extraction scheme. We have a net of interest for which we would like to extract the capacitance (Fig.10). We have already computed the coupling between the NOI and the left lateral neighbor, and we have discovered that the neighbor on the right will make a small but not negligible difference in the capacitance of the NOI. We try using the technique outlined above and use a transformed low-accuracy model for the right neighbor (Fig.10d). We compare the results with those of higher accuracy. To emphasize the necessity of the new technique, we also do the extraction using low accuracy models for all three elements (Fig.10e). We see that the proposed technique is a good compromise between computational cost and accuracy because it provides accuracy only where needed. Note that the percentage error for the mixed extraction (Fig.10d) for the coupling between the NOI and the right lateral neighbor is roughly equal to the error of the same for the extraction with coarse elements (Fig.10e). This is to be expected because the transformation does not increase the accuracy of the coarse model used. If we use the relative error measure:

$$E(C_{ij}^{\mathrm{n1}}) = \frac{C_{ij}^{\mathrm{n1}} - C_{ij}^{0}}{C_{ii}^{0}} \tag{17}$$

which is more meaningful in the net-by-net extraction context, we see that indeed we have good overall accuracy for the column corresponding to the NOI (2nd column) compared to the coarse extrac-

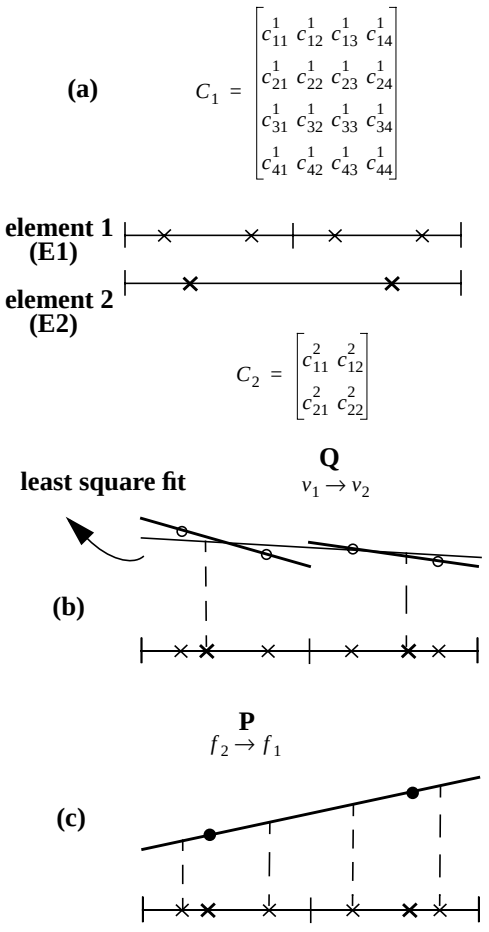

Figure 8. Matching elements with different discretization. (a) The elements are represented by their capacitance macromodel matrices, which have different sizes. (b) The potential on element 1 is mapped onto the potential on element 2. (c) The flux density on element 2 is mapped onto the flux density on element 1.

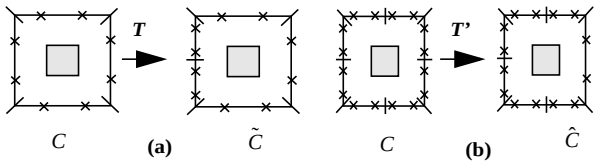

Figure 9. Transforming elements: (a) The matrix transformation *T* creates a new *version* of an element by increasing the discretization on one (or more) of the edges; (b) The matrix transformation *T'* creates a new *version* of an element by decreasing the discretization on one (or more) of the edges.

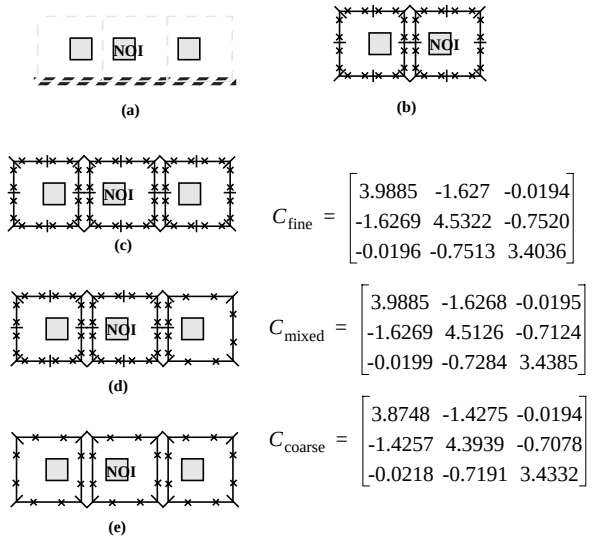

Figure 10. Example to illustrate the accuracy of mixing elements of different discretizations: (a) shows the configuration and the decomposition into elements – in this case, three instances of one unique library element; (b) shows the initial extraction, taking into account only the NOI and the left lateral neighbor; (c) shows the resulting capacitance matrix when only elements with high discretization are used; (d) shows the use of mixed elements; (e) shows the solution using only elements with coarse discretization.

tion:

$$\Delta C^{\text{rel}}_{\text{mixed}} = \begin{bmatrix} -1\times10^{-7} & 3\times10^{-5} & 2\times10^{-5} \\ 7\times10^{-7} & -0.0043 & 0.0116 \\ -9\times10^{-5} & 0.0051 & 0.0102 \end{bmatrix},$$

$$\Delta C^{\text{rel}}_{\text{coarse}} = \begin{bmatrix} 0.0285 & -0.0440 & 3\times10^{-5} \\ -0.0505 & 0.0262 & -0.0014 \\ 0.0005 & -0.0020 & 0.0016 \end{bmatrix}. \quad (18)$$

There also exists the dual transformation, which we shall call $\boldsymbol{T}'$. We define the new transformation:

$$\boldsymbol{T}' : C_2^{(4\times4)} \rightarrow Q^{(2\times4)} C_2^{(4\times4)} P^{(4\times2)} = \hat{C}_2, \quad (19)$$

where this time $\boldsymbol{P}$ interpolates the *potential* and $\boldsymbol{Q}$ performs a least-squares fit to match the *flux density* (Fig. 9(b)). We can use the dual transformations together to our advantage. We can use $\boldsymbol{T}$ when we need an element with only one accurate edge, and $\boldsymbol{T}'$ when we need one with only one coarse edge.

6. Conclusion

The Boundary Element Method implementation of the 2-D hierarchical field solution technique introduced in [3] is more efficient than the Finite Difference implementation. Among many options available for the BEM implementation, the choice of linear discontinuous elements seems to offer a good compromise between efficiency and accuracy. Parameterized elements allow the analysis of gridless designs with reasonable accuracy and a small library size. A pair of linear transformations allow us to use elements with different discretizations together. Using these transformations, elements with lower accuracy can be used where high accuracy is not required, resulting in further gains in efficiency.

7. Bibliography

[1] Anand, M.B. *et al.* "Fully Integrated Back End of the Line Interconnect Process," *1994 VLSI Multilevel Interconnect Conference*, June 7-8, 1994, IEEE 1994 pp. 15-21

[2] Brebbia, C.A; Telles, J.C.F; Wrobel, L.C. *Boundary Element Techniques*, Springer-Verlag, Berlin, Heidelberg, 1984

[3] Dengi, E.A.; "A Parasitic Capacitance Extraction Method for VLSI Interconnect Modeling", PhD Thesis, Carnegie Mellon University, March 1997

[4] Dengi, E.A.; Rohrer, R.A.; "Hierarchical 2-D Field Solution for Capacitance Extraction for VLSI Interconnect Modeling", *to appear at 34th Design Automation Conference*, Anaheim, CA, June 9-13, 1997

[5] Fukuda, S; Shigyo, N; Kato, K; Nakamura, S. "A ULSI 2-D Capacitance Simulator for Complex Structures Based on Actual Processes," *IEEE Trans. Computer-Aided Design*, TCAD-9 no.1, pp.39-47, Jan. 1990

[6] Gray, L.J; Lutz, E. "On the treatment of corners in the boundary element method," *J. Comput. Appl. Math.* Vol. 32, pp. 369-386, 1990

[7] Kane, J.H; Kumar, B.L.K; Saigal, S. "An Arbitrary Condensing, Noncondensing Solution Strategy for Large Scale, Multizone Boundary Element Analysis," *Computer Meth. Appl. Mech. Eng.* 79(1990) pp. 219-244

[8] Patterson, C; Sheikh, M.A. "Interelement continuity in the boundary element method," in *Topics in Boundary Element Research, Vol. 1,* C.A. Brebbia (ed.), Springer-Verlag, Berlin, 1984

[9] Ruehli, A.E; Brennan, P.A. "Efficient Capacitance Calculations for Three Dimensional Multiconductor Systems," *IEEE Trans. Microwave Theory Tech.* MTT-21, pp. 76-82, 1973

[10] Wendland, W.L; Yu, D. "Adaptive boundary element methods for strongly elliptic integral equations," *Numer. Math.*, Vol. 53, pp. 539-558, 1988

[11] Yan, G; Lin, F. "Treatment of corner node problems and its singularity," *Engineering Analysis with Boundary Elements* Vol.13, pp.75-81, 1994